

Phosphonoacetic acid as a building block in supramolecular chemistry: salts with organic polyamines

Katharine F. Bowes,^a George Ferguson,^{a,b} Alan J. Lough,^c Choudhury M. Zakaria^{a†} and Christopher Glidewell^{a*}

^aSchool of Chemistry, University of St Andrews, St Andrews, Fife KY16 9ST, UK, ^bDepartment of Chemistry and Biochemistry, University of Guelph, Ontario N1G 2W1, Canada, and ^cLash Miller Chemical Laboratories, University of Toronto, Ontario M5S 3H6, Canada

† On leave from Department of Chemistry, University of Rajshahi, Rajshahi, Bangladesh

Correspondence e-mail: cg@st-andrews.ac.uk

Phosphonoacetic acid, (HO)₂P(O)CH₂COOH, forms adducts with a range of amines. The acid component in these adducts may be the neutral molecule C₂H₅O₅P, the mono-anion (C₂H₄O₅P)[−] or the di-anion (C₂H₃O₅P)^{2−}. The substructure formed by the acid component takes the form of simple chains in compounds (1)–(3), which are the 1:1 adducts formed with 1,4-diazabicyclo[2.2.2]octane, 4,4'-bipyridyl and 1,3-trimethylenedipiperidine, respectively. These adducts contain C₂H₅O₅P, (C₂H₄O₅P)[−] and (C₂H₃O₅P)^{2−}, respectively, although (3) is solvated by a mixture of methanol and water. The (C₂H₄O₅P)[−] anion substructure in (4), which is the adduct formed with *meso*-5,5,7,12,12,14-hexa-*C*-methyl-1,4,8,11-tetraazacyclotetradecane, is a chain of spiro-fused rings, while the substructure in (5), which is the adduct formed with 2,2'-dipyridylamine, is a chain of edge-fused rings. In (6), the adduct formed with 1,2-bis(4'-pyridyl)ethane, the anion substructure is two-dimensional. The chain substructures are linked by the amine units into two-dimensional structures in (1) and (4) and into three-dimensional frameworks in (2), (3) and (5), while the anion sheets in (6) are likewise linked by the amine units into a three-dimensional framework.

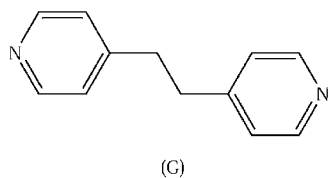
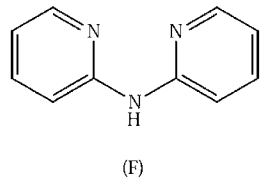
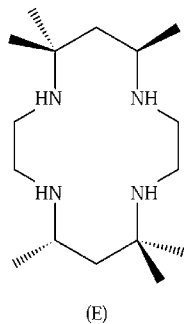
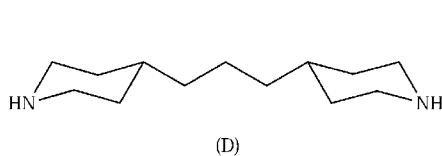
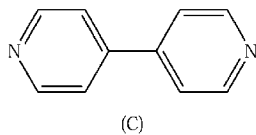
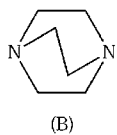
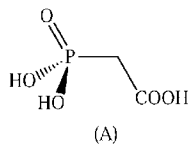
Received 1 July 2002

Accepted 6 September 2002

1. Introduction

Although only a few structures have been reported of salts that contain the mono-anion C₂H₄O₅P[−], which is derived from phosphonoacetic acid, (HO)₂P(O)CH₂COOH, it is clear that this anion is potentially an extremely versatile building block in supramolecular chemistry. In the neutral acid itself, the three-dimensional structure is built from C(4) and C(6) helical chains in space group *P*₂₁₂₁, so that small rings are completely absent (Lis, 1997). In this respect, the behaviour of phosphonoacetic acid differs markedly from that of phenylphosphonic acid, PhP(O)(OH)₂ (Weakley, 1976), where it is possible to identify both R₂²(8) rings and C(4) chains, motifs that dominate the aggregation patterns found in salts of the anion [PhP(O)₂OH][−] (Ferguson *et al.*, 1998). In the lithium salt of phosphonoacetic acid [Cambridge Structural Database (CSD; Allen & Kennard, 1993) refcode TERMOS; Lis, 1997], anions [(HO)P(O)₂CH₂COOH][−] are linked into chains that contain alternating R₂²(8) rings, which are formed by the phosphonate units, and R₂²(12) rings, which are formed by a carboxyl donor and phosphonate acceptors. In these chains, the R₂²(8) and R₂²(12) rings are linked in spiro fashion at the P atoms; despite the presence of un-ionized carboxyl groups, the characteristic R₂²(8) carboxyl dimer motif is absent. In the 1:2 salt [(MeNH(CH₂CH₂)₂NHMe)²⁺]₂·[(C₂H₄O₅P)[−]]₂ formed with *N,N'*-dimethylpiperazine (Farrell *et al.*, 2001), all of the H-atom sites that are bonded to O atoms have 0.5 occupancy at 293 (2) K, and the anions are linked into sheets of alternating R₂²(12) and R₆⁶(28) rings. This salt contains no R₂²(8)

rings at all, and the $R_2^2(12)$ rings contain phosphonic donors and carboxyl acceptors, in contrast to the corresponding rings in the Li salt (Lis, 1997).



In a continuation of our study of the amine salts formed by phosphonoacetic acid (Farrell *et al.*, 2001), we have now synthesized and characterized the salt-type adducts formed by this acid (*A*; see scheme above) with each of 1,4-diazabicyclo[2.2.2]octane (DABCO) (*B*), 4,4'-bipyridyl (*C*), 1,3-trimethylenedipiperidine (*D*), tet-*a* (*meso*-5,5,7,12,12,14-hexamethyl-1,4,8,11-tetraazacyclotetradecane, $C_{16}H_{36}N_4$) (*E*), 2,2'-dipyridylamine (*F*) and 1,2-bis(4'-pyridyl)ethane (*G*). The resulting adducts have the compositions $(C_6H_{12}N_2) \cdot (C_2H_5O_5P)$ [1; 1,4-diazabicyclo[2.2.2]octane–phosphonoacetic acid (1/1)], $(C_{10}H_8N_2) \cdot (C_2H_5O_5P)$ [2; 4,4'-bipyridyl–phosphonoacetic acid (1/1)], $(C_{13}H_{26}N_2) \cdot (C_2H_5O_5P) \cdot (CH_4O)_{0.352} \cdot (H_2O)_{0.788}$ [3; 1,3-trimethylenedipiperidine–phosphonoacetic acid (1/1) methanol/water solvate], $(C_{16}H_{36}N_4) \cdot (C_2H_5O_5P)_2$ [4; tet-*a*–phosphonoacetic acid (1/2)], $(C_{10}H_9N_3) \cdot (C_2H_5O_5P)$ [5; 2,2'-dipyridylamine–phosphonoacetic acid (1/1)], $(C_{12}H_{12}N_2) \cdot (C_2H_5O_5P)_2$ [6; 1,2-bis(4'-pyridyl)ethane–phosphonoacetic acid (1/2)].

2. Experimental

2.1. Syntheses

Equimolar quantities of the appropriate amine and the acid were separately dissolved in methanol. The solutions were

mixed, then the mixtures were set aside to crystallize, and they yielded (1)–(6). Analyses: (1) found C 37.7, H 4.9, N 10.6; $C_8H_{17}N_2O_5P$ requires C 38.1, H 6.8, N 11.1%; (2) found C 49.0, H 4.0, N 9.4; $C_{12}H_{12}N_2O_5P$ requires C 48.7, H 4.4, N 9.5%; (3) consistent analysis not obtained; $C_{30}H_{62}N_4O_{10}P_2$ requires C 51.4, H 8.9, N 8.0%; $C_{30.70}H_{67.96}N_4O_{12.28}P_2$ (from X-ray analysis) requires C 49.0, H 9.1, N 7.5%; (4) found C 42.4, H 8.3, N 9.7; $C_{20}H_{46}N_2O_{10}P_2$ requires C 42.5, H 8.2, N 9.9%; (5) found C 46.5, H 4.3, N 13.5; $C_{12}H_{14}N_3O_5P$ requires C 46.3, H 4.5, N 13.5%; (6) found C 41.5, H 4.1, N 6.0; $C_{16}H_{22}N_2O_{10}P_2$ requires C 41.4, H 4.8, N 6.0%. Crystals suitable for single-crystal X-ray diffraction were selected directly from the analytical samples.

2.2. Data collection, structure solution and refinement

Diffraction data for (1)–(6) were collected at 150 (1) K using a Nonius Kappa-CCD diffractometer with graphite-monochromated Mo $K\alpha$ radiation ($\lambda = 0.71073 \text{ \AA}$). Other details of cell data, data collection and refinement are summarized in Table 1. The following software was employed: *PRPKAPPA* (Ferguson, 1999), *Kappa-CCD* (Nonius, 1997), *DENZO-SMN* (Otwinowski & Minor, 1997), *SHELXL97* (Sheldrick, 1997a), *SHELXS97* (Sheldrick, 1997b), *PLATON* (Spek, 2003).

For (2) the space group $P2_1/n$ was uniquely assigned from the systematic absences: space group $P2_1/c$ was similarly assigned for (6). Compounds (3), (4) and (5) are all triclinic: in each case space group $P\bar{1}$ was chosen and confirmed by the successful structure analysis. For (1), the systematic absences permitted $Pca2_1$ and $Pcam$ (= $Pbcm$, No. 57) as possible space groups: $Pca2_1$ was selected and confirmed by the successful analysis. The structures were solved by direct methods and refined with all data on F^2 . A weighting scheme based on $P = (F_o^2 + 2F_c^2)/3$ was employed in order to reduce statistical bias (Wilson, 1976). The asymmetric unit in (3) contains two cations, two anions, three water molecules with partial occupancies and one methanol with partial occupancy; the occupancies refined to the values water O71 0.297 (9), methanol O81 C82 0.703 (9), water O91 0.434 (15), water O92 0.845 (19). No allowance was made for H atoms on the molecules with partial occupancy. The cations in each of (4) and (6) lie across inversion centres. In (4), the cation exhibits some disorder of the axial methyl groups with the groups containing C52 and C72 having site-occupation factors of 0.711 (4) and 0.289 (4), respectively. This behaviour is most readily interpreted in terms of a 180° rotation of the cation, in a fraction of the sites, about a line joining the mid-points of the C2–C3 and C2ⁱ–C3ⁱ bonds [$i = (1 - x, 1 - y, 1 - z)$]. Because of the small partial occupancy of C72, an apparently short intermolecular C72ⁱ...C72ⁱⁱ [$ii = (1 - x, -y, 1 - z)$] contact of 2.639 (10) Å may be ignored. The cation in (5) exhibits orientational disorder and the location of the amino N was modelled over two sites (denoted N1 and N1A) with site-occupation factors of 0.916 (4) and 0.084 (4): possibly because of the very low occupancy of the minor orientation, it was not possible to determine coordinates for the C atoms of the

Table 1
Experimental details.

	(1)	(2)	(3)	(4)	(5)	(6)
Crystal data						
Chemical formula	C ₆ H ₁₂ N ₂ ·- C ₂ H ₅ O ₅ P	C ₁₀ H ₉ N ₂ ·- C ₂ H ₄ O ₅ P	2(C ₁₃ H ₂₈ N ₂)·- 2(C ₂ H ₅ O ₅ P)·- 1.58(H ₂ O)·- 0.70(CH ₄ O)	C ₁₆ H ₃₈ N ₄ ·- 2(C ₂ H ₄ O ₅ P)	C ₁₀ H ₁₀ N ₃ ·- C ₂ H ₄ O ₅ P	C ₁₂ H ₁₄ N ₂ · 2(C ₂ H ₄ O ₅ P)
Chemical formula weight	252.21	296.21	745.67	564.55	311.23	464.3
Cell setting, space group	Orthorhombic, <i>Pca</i> 2 ₁	Monoclinic, <i>P</i> 2 ₁ / <i>n</i>	Triclinic, <i>P</i> $\bar{1}$	Triclinic, <i>P</i> $\bar{1}$	Triclinic, <i>P</i> $\bar{1}$	Monoclinic, <i>P</i> 2 ₁ / <i>c</i>
<i>a</i> , <i>b</i> , <i>c</i> (Å)	20.3011 (17), 6.7692 (5), 8.0158 (6)	4.6225 (2), 17.2421 (6), 15.6529 (7)	11.7486 (3), 13.3913 (4), 13.8206 (5)	8.7219 (2), 9.8947 (1), 9.9343 (2)	7.0706 (2), 10.6500 (3), 10.7020 (4)	8.8501 (3), 15.1862 (6), 7.3741 (3)
α , β , γ (°)	90, 90, 90	90, 95.7190 (15), 90	96.9260 (17), 109.4140 (16), 105.4830 (15)	62.5110 (9), 85.6800 (8), 67.1910 (9)	115.8690 (13), 98.8120 (15), 104.0040 (13)	90, 90.761 (2), 90
<i>V</i> (Å ³)	1101.55 (15)	1241.35 (9)	1923.2 (1)	695.42 (2)	671.96 (4)	990.99 (7)
<i>Z</i>	4	4	2	1	2	2
<i>D_x</i> (Mg m ⁻³)	1.521	1.585	1.288	1.348	1.538	1.556
Radiation type	Mo <i>K</i> α	Mo <i>K</i> α	Mo <i>K</i> α	Mo <i>K</i> α	Mo <i>K</i> α	Mo <i>K</i> α
No. of reflections for cell parameters	1987	2390	8765	2923	3079	5037
θ range (°)	3.6–25.5	2.6–27.5	3.1–27.6	2.6–27.4	3.1–27.6	2.7–27.5
μ (mm ⁻¹)	0.259	0.244	0.176	0.213	0.232	0.279
Temperature (K)	150 (1)	150 (1)	150 (1)	150 (1)	150 (1)	150 (1)
Crystal form, colour	Plate, colourless	Block, colourless	Plate, colourless	Needle, colourless	Plate, colourless	Plate, colourless
Crystal size (mm)	0.18 × 0.10 × 0.03	0.34 × 0.20 × 0.15	0.16 × 0.10 × 0.06	0.40 × 0.24 × 0.20	0.34 × 0.16 × 0.16	0.28 × 0.12 × 0.08
Data collection						
Diffractometer	Kappa-CCD	Kappa-CCD	Kappa-CCD	Kappa-CCD	Kappa-CCD	Kappa-CCD
Data collection method	φ scans, and ω scans with κ offsets	φ scans, and ω scans with κ offsets	φ scans, and ω scans with κ offsets	φ scans, and ω scans with κ offsets	φ scans, and ω scans with κ offsets	φ scans, and ω scans with κ offsets
No. of measured, independent and observed reflections	7195, 1987, 1462	8078, 2824, 2194	24 179, 8765, 5307	9161, 3148, 2745	9556, 3079, 2471	6047, 2263, 1883
Criterion for observed reflections	<i>I</i> > 2σ(<i>I</i>)	<i>I</i> > 2σ(<i>I</i>)	<i>I</i> > 2σ(<i>I</i>)	<i>I</i> > 2σ(<i>I</i>)	<i>I</i> > 2σ(<i>I</i>)	<i>I</i> > 2σ(<i>I</i>)
<i>R</i> _{int}	0.119	0.034	0.108	0.026	0.056	0.035
θ _{max} (°)	25.5	27.5	27.6	27.4	27.6	27.5
Range of <i>h</i> , <i>k</i> , <i>l</i>	-21 → <i>h</i> → 24 -8 → <i>k</i> → 8 -9 → <i>l</i> → 9	0 → <i>h</i> → 6 0 → <i>k</i> → 22 -20 → <i>l</i> → 20	-15 → <i>h</i> → 15 -17 → <i>k</i> → 17 -17 → <i>l</i> → 17	0 → <i>h</i> → 11 -11 → <i>k</i> → 12 -12 → <i>l</i> → 12	-9 → <i>h</i> → 9 -13 → <i>k</i> → 13 -13 → <i>l</i> → 13	-11 → <i>h</i> → 11 -19 → <i>k</i> → 19 -9 → <i>l</i> → 9
Refinement						
Refinement on <i>R</i> [[<i>F</i> ² > 2σ(<i>F</i> ²)], <i>wR</i> (<i>F</i> ²), <i>S</i>]	<i>F</i> ² 0.055, 0.141, 1.02	<i>F</i> ² 0.039, 0.102, 1.03	<i>F</i> ² 0.080, 0.228, 1.03	<i>F</i> ² 0.036, 0.0978, 1.05	<i>F</i> ² 0.041, 0.110, 1.07	<i>F</i> ² 0.038, 0.103, 1.06
No. of reflections and parameters used in refinement	1987, 148	2824, 183	8765, 466	3148, 174	3079, 198	2263, 139
H-atom treatment	H-atom parameters constrained	H-atom parameters constrained	H-atom parameters constrained	H-atom parameters constrained	H-atom parameters constrained	H-atom parameters constrained
Weighting scheme	$w = 1/[\sigma^2(F_o^2) + (0.0527P)^2 + 0.0408P]$ where $P = (F_o^2 + 2F_c^2)/3$	$w = 1/[\sigma^2(F_o^2) + (0.0414P)^2 + 0.5382P]$ where $P = (F_o^2 + 2F_c^2)/3$	$w = 1/[\sigma^2(F_o^2) + (0.0954P)^2 + 1.4703P]$ where $P = (F_o^2 + 2F_c^2)/3$	$w = 1/[\sigma^2(F_o^2) + (0.0375P)^2 + 0.3032P]$ where $P = (F_o^2 + 2F_c^2)/3$	$w = 1/[\sigma^2(F_o^2) + (0.0437P)^2 + 0.2307P]$ where $P = (F_o^2 + 2F_c^2)/3$	$w = 1/[\sigma^2(F_o^2) + (0.0431P)^2 + 0.3391P]$ where $P = (F_o^2 + 2F_c^2)/3$
(Δ/σ) _{max}	0.016	0.001	0.000	0.000	0.000	0.001
$\Delta\rho_{max}$, $\Delta\rho_{min}$ (e Å ⁻³)	0.301, -0.525	0.259, -0.367	0.683, -0.433	0.273, -0.413	0.314, -0.359	0.308, -0.438
Extinction method	None	None	<i>SHELXL</i>	None	<i>SHELXL</i>	<i>SHELXL</i>
Extinction coefficient	0	0	0.028 (4)	0	0.015 (4)	0.011 (3)

minor orientation (all of these would be very close to the sites of the major-form C atoms). All full-occupancy H atoms were located from difference maps and included in the refinements as riding atoms with distances O—H 0.82–0.84 Å, N—H 0.88–0.93 Å and C—H 0.92–1.00 Å. For (1) the anomalous dispersion terms are on the borderline of being significant (heaviest atom P); Friedel reflections were not merged and refinement with 988 Friedel pairs led to a Flack value of 0.1 (2), which does not really allow any meaningful comment.

The diagrams were prepared with the aid of *PLATON* (Spek, 2003). Details of hydrogen-bond dimensions and of molecular conformations are given in Tables 2 and 3. Figs. 1–18 show the molecular components, with the atom-labelling schemes and aspects of the supramolecular structures.¹

3. Results and discussion

3.1. Compositions and molecular constitutions

Compounds (1), (2) and (5) all have 1:1 stoichiometry, while in each of (4) and (6) the ratio of amine to acid components is 1:2. Compound (3) is also solvated with partial-occupancy methanol and water molecules present, thus $(C_{13}H_{28}N_2) \cdot (C_2H_5O_5P) \cdot (H_2O)_{0.79} \cdot (CH_4O)_{0.35}$. A consistent elemental analysis could not be obtained for this material, possibly because the bulk preparation is actually a mixture of several different partial solvates. This assumption would in turn be consistent with the structural findings (see §3.3.2, below) that neither of the solvent components plays a significant role in the formation of the supramolecular structure. In (1), both of the independent molecular components are overall neutral with no proton transfer from the acid to the base. Of the remainder, the majority are simple salts in which one or, in the case of (3) only, two protons have been completely transferred from the phosphonic acid to the amine.

The H transfer is complete in (2)–(6), in contrast to the behaviour in the salt formed with *N,N'*-dimethylpiperazine (Farrell *et al.*, 2001), where all of the H-atom sites that are bonded to O atoms have 0.5 occupancy at 293 (2) K.

3.2. Molecular conformations

3.2.1. Amine components. The leading torsional and dihedral angles are given in Table 3. In (1) the N—C—C—N torsional angles in the DABCO component indicate only a very modest deviation from the idealized D_{3h} ($\bar{6}m2$) molecular symmetry; the twist of the molecule from D_{3h} symmetry may be regarded as an internal rotation about the N···N vector, while in the D_{3h} conformation, the neighbouring CH₂ groups are all eclipsed. For isolated DABCO molecules in the gas phase (Yokozeki & Kuchitsu, 1971) the internal dynamics indicate a very broad potential well for the twist motion, which is best fitted by a harmonic quartic potential function that has an energy minimum that corresponds to a twist of *ca.* 10° from

¹ Lists of atomic coordinates, anisotropic displacement parameters, geometric parameters and structure factors have been deposited with the IUCr (Reference: BM0057). Services for accessing these data are described at the back of the journal.

Table 2
Hydrogen-bond parameters (Å, °).

<i>D</i> —H··· <i>A</i>	H··· <i>A</i>	<i>D</i> ··· <i>A</i>	<i>D</i> —H··· <i>A</i>
(1)			
O1—H1···N1	1.79	2.605 (5)	164
O3—H3···O5 ⁱ	1.74	2.538 (5)	157
O4—H4···N2 ⁱⁱ	2.00	2.606 (5)	129
(2)			
O1—H1A···N2	1.81	2.645 (2)	176
O3—H3···O4 ⁱⁱⁱ	1.70	2.515 (2)	162
N1—H1···O5 ^{iv}	1.74	2.582 (2)	158
C12—H12···O2 ^{iv}	2.22	2.978 (2)	135
C13—H13···O3 ^v	2.46	3.369 (2)	159
C15—H15···O4 ^{vi}	2.36	3.269 (2)	153
C26—H26···O1 ^{vii}	2.54	3.430 (2)	155
(3)			
N11—H11A···O22	1.81	2.716 (5)	168
N11—H11B···O12	1.83	2.659 (5)	149
N21—H21A···O14 ^{viii}	2.08	2.806 (4)	134
N21—H21B···O14 ^{ix}	1.81	2.722 (4)	174
N31—H31A···O21	2.34	2.834 (4)	113
N31—H31A···O25	2.01	2.840 (4)	150
N31—H31B···O15	1.90	2.797 (4)	166
N41—H41A···O24 ^x	1.81	2.721 (4)	171
N41—H41B···O24 ^{xi}	2.12	2.976 (4)	154
O13—H13···O21	1.70	2.533 (4)	171
O23—H23···O11 ⁱⁱⁱ	1.72	2.524 (4)	160
(4)			
N1—H11A···N4 ^{vii}	2.08	2.817 (2)	137
O1—H1···O5 ^{xiii}	1.69	2.517 (2)	167
O3—H3···O4 ^{xiii}	1.74	2.581 (2)	174
N1—H1B···O4	1.91	2.799 (2)	160
N4—H4···O1 ⁱⁱⁱ	2.57	3.428 (2)	155 [†]
N4—H4···O2 ^{vii}	2.56	3.198 (2)	127 [†]
C2—H2A···O5 ⁱⁱⁱ	2.50	3.426 (2)	156
(5)			
N12—H12···N22	1.97	2.632 (2)	131
O1—H1A···O5 ^{xiv}	1.76	2.570 (2)	163
O3—H3···O4 ^{vii}	1.80	2.604 (2)	161
N1—H1···O4	1.87	2.743 (2)	171
N12—H12···O5	2.34	3.062 (2)	140
C24—H24···O2 ^{xv}	2.53	3.312 (3)	140
C26—H26···O2 ^{vii}	2.48	3.201 (3)	132
(6)			
O1—H1···O4 ^{vii}	1.81	2.640 (2)	169
O3—H3···O5 ^{xvi}	1.71	2.521 (2)	163
N11—H11···O4	1.73	2.613 (2)	178
C13—H13···O3 ^{xvii}	2.52	3.349 (2)	146
C15—H15···O3 ^{xviii}	2.48	3.329 (2)	148
C16—H16···O2 ^{vii}	2.38	3.256 (2)	154

[†] Three-centre N—H···(O)₂ system: sum of angles at H4, 358°. Symmetry codes: (i) $\frac{2}{3}-x, y, \frac{1}{2}+z$; (ii) $\frac{1}{2}+x, -y, z$; (iii) $1+x, y, z$; (iv) $\frac{2}{3}-x, \frac{1}{2}+y, \frac{1}{2}-z$; (v) $2-x, 1-y, 1-z$; (vi) $\frac{2}{3}+x, \frac{1}{2}-y, -\frac{1}{2}+z$; (vii) $1-x, 1-y, 1-z$; (viii) $x, -1+y, -1+z$; (ix) $-x, -y, -z$; (x) $1-x, 2-y, 1-z$; (xi) $x, 1+y, 1+z$; (xii) $-x, 1-y, 1-z$; (xiii) $-x, 2-y, -z$; (xiv) $-1+x, y, z$; (xv) $1+x, y, 1+z$; (xvi) $x, \frac{1}{2}-y, -\frac{1}{2}+z$; (xvii) $1-x, -\frac{1}{2}+y, \frac{1}{2}-z$; (xviii) $-1+x, \frac{1}{2}-y, \frac{1}{2}+z$.

the D_{3h} geometry. With this twist motion in mind, it is of interest to compare the conformation in (I) with that in the related adduct formed with *N*-(phosphonomethyl)imino-diacetic acid, where the mean N—C—C—N torsional angle is much larger at -17.2 (2)° (Bowes *et al.*, 2002).

The 4,4'-bipyridyl and 2,2'-dipyridylamine units in (2) and (5), respectively, are nearly planar, whereas the pyridyl rings in the amine component of (6) are almost orthogonal to the planar central C—C—C unit (Fig. 15). The conformational differences between the diamine units in (2) and (6) may be heavily influenced by the different patterns of the C—H···O

Table 3
Selected torsional and dihedral angles (°).

<i>(a)</i> Amine components			
(1)			
N1—C11—C21—N2	2.8	(6)	
N1—C12—C22—N2	3.1	(6)	
N1—C13—C23—N2	3.0	(6)	
(2)			
(N1, C12—C16)			
∧(N2, C22—C26)	5.5	(2)	
(3)			
C16—C15—C14—C17	−177.3	(3)	C32—C33—C34—C37 175.5 (3)
C15—C14—C17—C18	175.2	(3)	C33—C34—C37—C38 166.6 (3)
C14—C17—C17—C27	−173.5	(3)	C34—C37—C38—C47 177.4 (3)
C17—C18—C27—C24	−177.4	(3)	C37—C38—C47—C44 169.5 (3)
C18—C27—C24—C23	179.3	(3)	C38—C47—C44—C45 −174.1 (3)
C27—C24—C23—C22	−179.8	(3)	C47—C44—C45—C46 178.8 (3)
(4)			
N1—C2—C3—N4	−69.3	(2)	C5—C6—N7—N1 ⁱ −71.1 (2)
C2—C3—N4—C5	−176.2	(2)	C6—C7—N1 ⁱ —C2 ⁱ 173.6 (2)
C3—N4—C5—C6	−174.4	(2)	C7—N1 ⁱ —C2 ⁱ —C3 ⁱ −175.0 (2)
N4—C5—C6—C7	63.3	(2)	
(5)			
C11—N1—C21—N22	6.7	(3)	C21—N1—C11—N12 −9.3 (3)
(6)			
C13—C14—C17—C17 ⁱⁱ	−92.4	(2)	
<i>(b)</i> Acid components†			
(1)			
O3—P1—C2—C1	−176.8	(3)	P1—C2—C1—O1 83.1 (5)
O4—P1—C2—C1	−58.5	(4)	P1—C2—C1—O2 −95.8 (5)
O5—P1—C2—C1	67.9	(4)	
(2)			
O3—P1—C2—C1	58.7	(2)	P1—C2—C1—O1 −107.2 (2)
O4—P1—C2—C1	174.3	(2)	P1—C2—C1—O2 72.2 (2)
O5—P1—C2—C1	−60.3	(2)	
(3)			
O13—P1—C2—C1	66.4	(3)	O23—P2—C4—C3 −177.6 (3)
O14—P1—C2—C1	−49.0	(3)	O24—P2—C4—C3 −60.5 (3)
O15—P1—C2—C1	−175.2	(3)	O25—P2—C4—C3 66.9 (3)
P1—C2—C1—O11	91.8	(4)	P2—C4—C3—O21 −85.0 (4)
P1—C2—C1—O12	−87.9	(4)	P2—C4—C3—O22 93.7 (4)
(4)			
O3—P1—C12—C11	−167.9	(2)	P1—C12—C11—O1 121.5 (2)
O4—P1—C12—C11	74.9	(2)	P1—C12—C11—O2 −57.4 (2)
O5—P1—C12—C11	−52.9	(2)	
(5)			
O3—P1—C2—C1	−77.6	(2)	P1—C2—C1—O1 −105.4 (2)
O4—P1—C2—C1	40.3	(2)	P1—C2—C1—O2 73.8 (2)
O5—P1—C2—C1	166.4	(2)	
(6)			
O3—P1—C2—C1	77.4	(2)	P1—C2—C1—O1 83.9 (2)
O4—P1—C2—C1	−39.9	(2)	P1—C2—C1—O2 −96.3 (2)
O5—P1—C2—C1	−164.5	(2)	

† Phosphonate O3 [O13 and O23 in (3)] carries H in all of (1)–(6); carboxyl O1 carries H in (1), (2) and (4)–(6). Symmetry codes: (i) $1-x, 1-y, 1-z$; (ii) $-x, -y, 1-z$.

hydrogen bonds, while the intramolecular N—H···N hydrogen bond in the 2,2'-dipyridylamine units of (5) certainly contributes to the planarity. In the cations of (3), both of the $\text{=}(CH_2)_3\text{=}$ spacer units have extended-chain conformations (Fig. 6), while the $[(\text{tet-}a)H_2]^{2+}$ cation in (4) adopts the usual *trans*-III configuration (Barefield *et al.*, 1986).

3.2.2. Acid components. In all of the compounds studied here, one of the phosphonate O atoms is antiperiplanar to the carboxyl C atom (C1): in the neutral acid component in (1), there is an OH unit antiperiplanar to C1, just as there is in the pure neutral acid itself (Lis, 1997). In the anions of (2), (3), (5)

and (6), and in the type 1 anion of (3), there is a negatively charged O atom antiperiplanar to C1, with the same conformation as that found previously in $\text{Li}[\text{C}_2\text{H}_4\text{O}_5\text{P}]$, in both polymorphs of $\text{K}[\text{C}_2\text{H}_4\text{O}_5\text{P}]\cdot\text{H}_2\text{O}$, in $[\text{NH}_4][\text{C}_2\text{H}_4\text{O}_5\text{P}]$ and in $\text{K}_2[\text{C}_2\text{H}_3\text{O}_5\text{P}]$ (Lis, 1997). By contrast, in (4) and in the type 2 anion of (3), the OH group of the phosphonate unit is antiperiplanar to C1.

3.3. Supramolecular structures

In all of the salts described in this paper, the ionic components are linked by an extensive series of hydrogen bonds (Table 2), which includes hard (Braga *et al.*, 1995) hydrogen bonds, mainly of the O—H···O and N—H···O types, with those of the O—H···N type occurring only in compounds (1) and (2) and those of the N—H···N type occurring only within the macrocyclic cation in compound (4). These hard hydrogen bonds are augmented in most compounds by soft hydrogen bonds, exclusively of the C—H···O type.

The analysis of the resulting supramolecular structures is greatly eased, in every case, by the use of the substructure approach (Gregson *et al.*, 2000). In each of (1)–(6), it is possible to identify a low-dimensional substructure that is formed by the phosphonic acid components alone, whether they are neutral or charged. These substructures are mostly one-dimensional, and they take the form of simple chains in (1), (2) and (3), a chain of spiro-fused rings in (4), and a molecular ladder, alternatively described as a chain of edge-fused rings, in (5). In (6) the anion substructure is two-dimensional. Consequently the structure descriptions below are based firstly on the formation of the phosphonic substructures and secondly on the manner in which these are linked by the cationic components by means of the hard hydrogen bonds; finally the effects of the soft C—H···O hydrogen bonds are analysed.

3.3.1. Neutral acid units form a simple chain. Both components of (1) (Fig. 1) are neutral and the phosphonic acid units form a *C*(4) chain motif. O3 in the acid molecule at (x, y, z) acts as hydrogen-bond donor to O5 at $(\frac{3}{2}-x, y, \frac{1}{2}+z)$, while O3 at $(\frac{3}{2}-x, y, \frac{1}{2}+z)$ in turn acts as hydrogen-bond donor to O5 at $(x, y, 1+z)$, and thus a zigzag chain along [001] is generated by the *c*-glide plane at $x = \frac{3}{4}$ (Fig. 2). A second similar chain, which is related to the first by the action of the 2_1 screw axis along $(\frac{1}{2}, y, 0)$, is generated by the *c*-glide plane at $y = \frac{1}{4}$. These chains are linked into (010) sheets by the DABCO units, which act as double acceptors in O—H···N hydrogen bonds.

Within the asymmetric unit (Fig. 1) N1 accepts a hydrogen bond from carboxyl O1. In the same DABCO unit at (x, y, z) , N2 accepts a hydrogen bond from O4 in the phosphonic acid unit at $(-\frac{1}{2}+x, -y, z)$. Propagation of these two O—H···N hydrogen bonds produces a $C_2^2(11)$ chain that runs parallel to the [100] direction and is generated by the *a*-glide plane at $y = 0$. Again, two of these chains run through each unit cell. The combination of [100] and [001] chains suffices to generate the sheets that are built from a single type of $R_6^0(30)$ ring (Fig. 2).

There are a number of intermolecular C—H···O contacts: all involve C—H bonds of rather low polarity in the neutral DABCO units, so that these interactions are expected to be quite weak. More importantly, all these bonds lie within a given (010) sheet, and hence there are no direction-specific

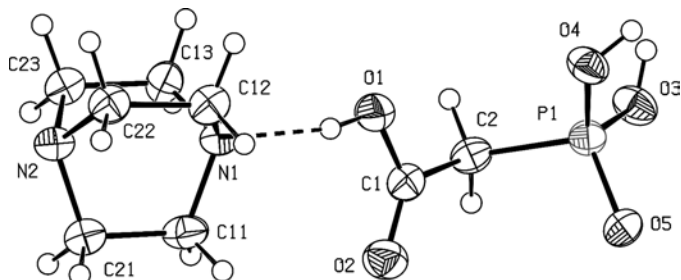


Figure 1
The molecular components of (1) and the atom-labelling scheme. Displacement ellipsoids are drawn at the 50% probability level.

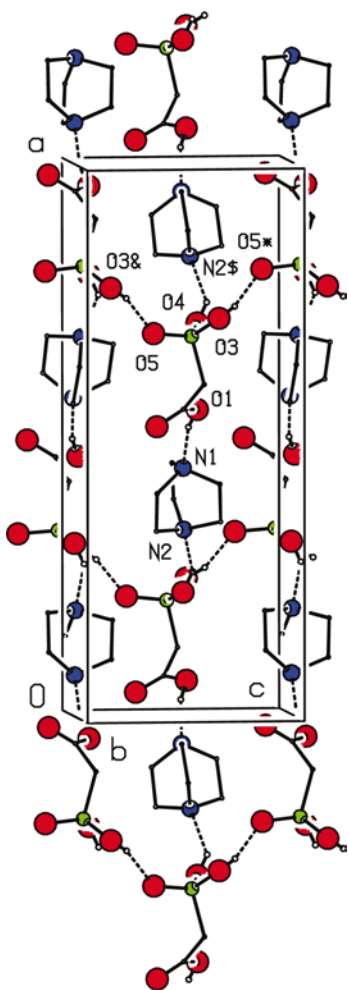


Figure 2
Part of the crystal structure of (1), which shows the formation of a (010) sheet built from $R_6^6(30)$ rings. For the sake of clarity, H atoms bonded to C atoms are omitted. The atoms marked with an asterisk (*), dollar sign (\$) or ampersand (&) are at the symmetry positions $(\frac{3}{2} - x, y, \frac{1}{2} + z)$, $(\frac{1}{2} + x, -y, z)$ and $(\frac{3}{2} - x, y, -\frac{1}{2} + z)$, respectively.

interactions between adjacent sheets, so that the supramolecular structure is strictly two dimensional.

3.3.2. The anions form simple chains. *Hard hydrogen bonds generate a two-dimensional structure.* In (2), the anion substructure takes the form of hydrogen-bonded C(4) chains that involve only the phosphonate groups. O3 in the anion at (x, y, z) acts as hydrogen-bond donor to O4 at $(1 + x, y, z)$, so a chain that runs parallel to the [100] direction is generated by translation.

The carboxyl O1 forms an O—H···N hydrogen bond within the asymmetric unit (Fig. 3) in which N2 acts as the acceptor.

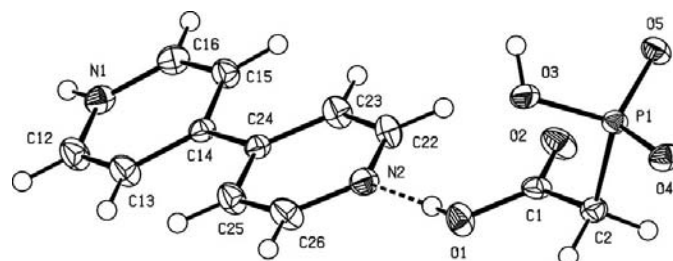


Figure 3
The molecular components of (2) and the atom-labelling scheme. Displacement ellipsoids are drawn at the 30% probability level.

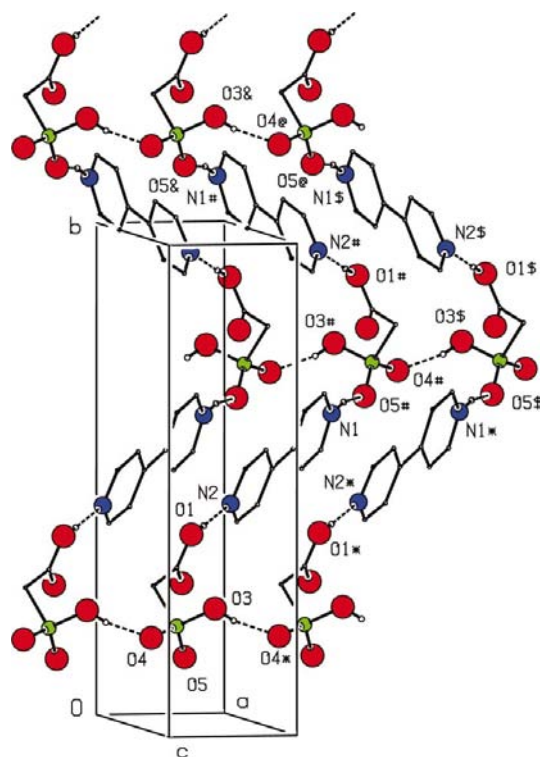


Figure 4
Part of the crystal structure of (2), which shows the formation of a (001) sheet built from $R_6^6(38)$ rings. For the sake of clarity, H atoms bonded to C atoms are omitted. The atoms marked with an asterisk (*), hash (#), dollar sign (\$), ampersand (&) or at sign (@) are at the symmetry positions $(1 + x, y, z)$, $(\frac{5}{2} - x, \frac{1}{2} + y, \frac{1}{2} - z)$, $(\frac{1}{2} - x, \frac{1}{2} + y, \frac{1}{2} - z)$, $(x, 1 + y, z)$ and $(1 + x, 1 + y, z)$, respectively.

The protonated N1 at (x, y, z) acts as hydrogen-bond donor to the phosphonate O5 at $(\frac{5}{2} - x, \frac{1}{2} + y, \frac{1}{2} - z)$, and N1 at $(\frac{5}{2} - x, \frac{1}{2} + y, \frac{1}{2} - z)$ in turn acts as donor to O5 at $(x, 1 + y, z)$. Hence a $C_2^2(15)$ chain that runs parallel to $[010]$ is generated by the 2_1 screw axis along $(\frac{5}{4}, y, \frac{1}{4})$. The combination of the $[100]$ and the $[010]$ chains generates a sheet parallel to (001) that is built from a single type of $R_6^6(38)$ ring (Fig. 4).

Two (001) sheets pass through each unit cell, which contains 2_1 screw axes at $z = \frac{1}{4}$ and $z = \frac{3}{4}$, respectively. Despite the rather

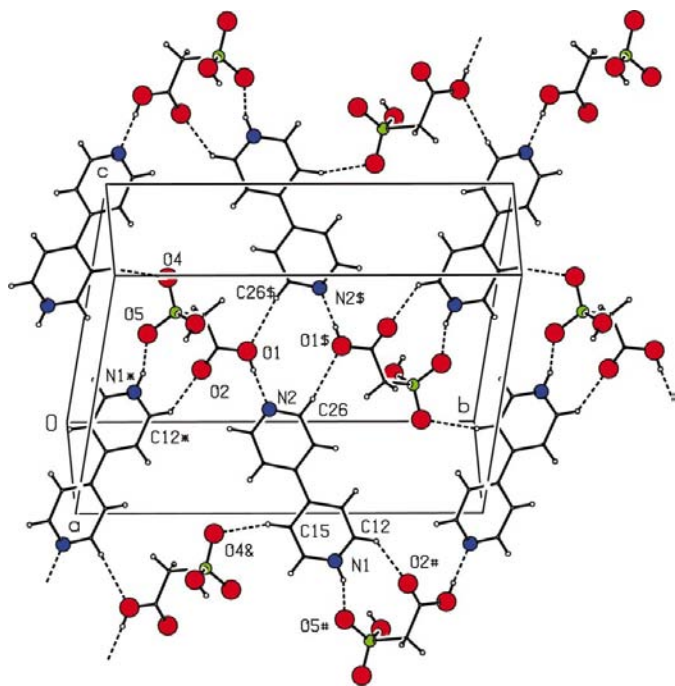


Figure 5

Part of the crystal structure of (2), which shows the linking by C—H...O hydrogen bonds of $[010]$ chains into a (103) sheet. The atoms marked with an asterisk (*), hash (#), dollar sign (\$) or ampersand (&) are at the symmetry positions $(\frac{5}{2} - x, -\frac{1}{2} + y, \frac{1}{2} - z)$, $(\frac{5}{2} - x, \frac{1}{2} + y, \frac{1}{2} - z)$, $(1 - x, 1 - y, 1 - z)$ and $(\frac{3}{2} + x, \frac{1}{2} - y, -\frac{1}{2} + z)$, respectively.

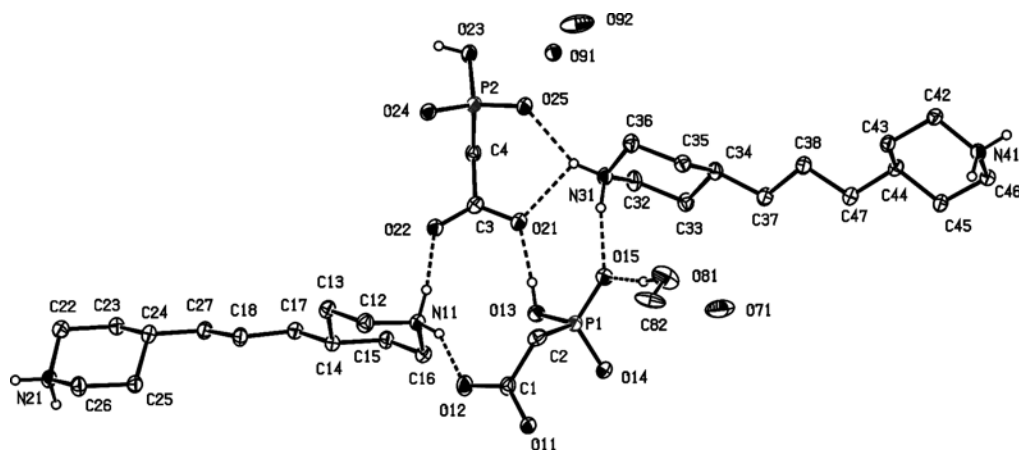


Figure 6

The molecular components of (3) and the atom-labelling scheme. Displacement ellipsoids are drawn at the 30% probability level. The methanol and water molecules all have partial occupancy, and their H atoms could not be located (see text).

large ring size within the sheets, adjacent sheets are not interwoven. Instead they are linked by a number of C—H...O hydrogen bonds, all of which involve C—H bonds in the cation (Table 2). Atom C15 in the cation at (x, y, z) , which lies in the $z = \frac{1}{4}$ sheet, acts as hydrogen-bond donor to O4 in the anion at $(\frac{3}{2} + x, \frac{1}{2} - y, -\frac{1}{2} + z)$, which is part of the $z = -\frac{1}{4}$ sheet: similarly C26 at (x, y, z) acts as donor to O1 in the anion at $(1 - x, 1 - y, 1 - z)$, which lies in the $z = \frac{3}{4}$ sheet. These two interactions link the $[010]$ chains into a (103) sheet (Fig. 5). Since there is also a C—H...O hydrogen bond within the $[010]$ chain (Table 2, Fig. 5), the (103) sheet consists of four different ring types, $R_2^2(9)$, $R_4^4(10)$, $R_4^4(16)$ and $R_4^4(24)$, the second and third of which are centrosymmetric. The final C—H...O hydrogen bond, which involves C13 as the donor, links adjacent (103) sheets in a further centrosymmetric motif. The combination of (001) sheets, which are generated exclusively by hard hydrogen bonds, and (103) sheets, which contain both hard and soft hydrogen bonds, suffices to form a continuous three-dimensional framework.

Hard hydrogen bonds generate a three-dimensional structure. The ionic components of (3) comprise two di-cations $[(\text{HNC}_5\text{H}_9\text{CH}_2\text{CH}_2\text{CH}_2\text{C}_5\text{H}_9\text{NH})^{2+}]$ and two di-anions $[(\text{C}_2\text{H}_3\text{O}_5\text{P})^{2-}]$, all of which lie in general positions in space group $P1$ together with partial methanol and water molecules, the latter distributed over several sites.

The two independent anions form a simple $C_2^2(12)$ chain that runs parallel to the $[100]$ direction. Within the asymmetric unit (Fig. 6), the phosphonate O13 acts as hydrogen-bond donor to the carboxylate O21, and the phosphonate O23 in the type 2 anion (containing P2) at (x, y, z) acts as donor to the carboxylate O11 in the type 1 anion (containing P1) at $(1 + x, y, z)$ (Fig. 7). Two such chains, which are related to one another by inversion and are hence of opposite polarities, pass through each unit cell. The chains of a given polarity and the two types of cation are linked by N—H...O hydrogen bonds to form $(01\bar{1})$ sheets in a two-dimensional substructure (Fig. 7), and these sheets are linked by further N—H...O hydrogen bonds into a three-dimensional framework. Note

that the one-dimensional and two-dimensional substructures are generated entirely by translation: only the linking of the $(01\bar{1})$ sheets involves the inversion operator.

The type 1 cation at (x, y, z) , which contains N11 and N21, acts as hydrogen-bond donor, *via* H11A and H11B, respectively, to the carboxylate O22 and O11 atoms in the two anions at (x, y, z) and, *via* H1A, to the phosphonate O14 atom in the type 1 anion at $(x, -1 + y, -1 + z)$. Similarly in the type 2 cation at (x, y, z) , which contains N31 and N41, N31 acts as donor, *via* H31A,

to both O21 and O25 in the type 2 anion at (x, y, z) , which interaction forms a planar three-centre $\text{N}-\text{H}\cdots(\text{O})_2$ system. N31 also acts as donor, *via* H31B, to O15 in the type 1 anion at (x, y, z) , while N41 acts as hydrogen-bond donor, *via* H41B, to the phosphonate O24 in the type 2 anion at $(x, 1 + y, 1 + z)$. Propagation of these $\text{N}-\text{H}\cdots\text{O}$ hydrogen bonds links the [100] anion chains into a $(01\bar{1})$ sheet (Fig. 7). Two sheets, which are related to one another by the action of the centres of inversion, pass through each unit cell, and adjacent sheets are linked into a single three-dimensional framework by two further $\text{N}-\text{H}\cdots\text{O}$ hydrogen bonds.

The two cations at (x, y, z) lie primarily in the reference $(01\bar{1})$ sheet (Fig. 7). However N21 and N41 at (x, y, z) act as hydrogen-bond donors, *via* H21B and H41A, respectively, to the phosphonate O14 and O24 atoms in the anions at $(-x, -y, -z)$ and $(1 - x, 2 - y, 1 - z)$, which form parts of the $(01\bar{1})$ sheets on either side of the reference sheet. In this manner a [021] chain is formed (Fig. 8) that directly links each sheet to the two neighbouring sheets, so forming a single three-dimensional structure.

The methanol molecule, whose site has only partial occupancy, is pendent from the framework but plays no part in its construction. Most likely the partial water molecules simply occupy spaces that would otherwise be empty.

3.3.3. The anions form a chain of spiro-fused rings. In the formation of the anion chain of (4) (Fig. 9), the carboxyl group is involved in addition to the phosphonate group (Table 2). The phosphonate O3 in the anion at (x, y, z) acts as hydrogen-bond donor to O4 in the anion at $(-x, 2 - y, -z)$, so a centrosymmetric $R_2^2(8)$ ring, which is centred at $(0, 1, 0)$, is generated. The carboxyl O1 in the anion at (x, y, z) acts as donor to the phosphonate O5 at $(-x, 1 - y, 1 - z)$, and hence a second centrosymmetric ring is formed, this time of $R_2^2(12)$

type and centred at $(0, \frac{1}{2}, \frac{1}{2})$. Propagation of these two hydrogen bonds by inversion thus generates a chain of rings, which are spiro-fused at the P atoms and run parallel to [011]. In this chain the $R_2^2(8)$ rings are centred at $(0, n, 1 - n)$ ($n = \text{zero or integer}$) and the $R_2^2(12)$ rings are centred at $(0, \frac{1}{2} + n, \frac{1}{2} - n)$ ($n = \text{zero or integer}$) (Fig. 10). Note that the centrosymmetric $R_2^2(8)$ ($-\text{COOH}$)₂ ring, which is so characteristic of simple carboxylic acids, is absent.

The [011] chains are linked into sheets by the centrosymmetric cations, in which each of the four axial $\text{N}-\text{H}$ bonds participates in the formation of intermolecular hydrogen bonds. Atom N1 is the donor in a two-centre $\text{N}-\text{H}\cdots\text{O}$ hydrogen bond, and N4 is the donor in an almost planar $\text{N}-\text{H}\cdots(\text{O})_2$ system, in which the two O acceptors lie in adjacent anions within a common chain (Table 2). Atom N1 at (x, y, z) , in the cation centred at $(\frac{1}{2}, \frac{1}{2}, \frac{1}{2})$, acts as hydrogen-bond donor, *via* the axial H1B, to the phosphonate O4 within the asymmetric unit (Fig. 9). Atom N4 at $(1 - x, 1 - y, 1 - z)$, which lies in the same $(\frac{1}{2}, \frac{1}{2}, \frac{1}{2})$ cation, acts as donor, *via* H4, both to the carboxyl O2 at (x, y, z) and to the carboxyl O1 at $(-x, 1 - y, 1 - z)$, both of which lie in the reference $[01\bar{1}]$ chain. In addition, N4 at (x, y, z) , within the same cation, acts as donor to O1 at $(1 + x, y, z)$ and to O2 at $(-x, 1 - y, 1 - z)$, which lie in an adjacent $[01\bar{1}]$ chain.

The anions at (x, y, z) and $(1 + x, y, z)$ are linked to generate a chain that runs parallel to [100], and the [100] and $[01\bar{1}]$ chains are combined to generate a sheet parallel to $(01\bar{1})$ (Fig. 11). Within the $(01\bar{1})$ sheet, each cation is linked to two chains and each adjacent pair of chains is linked by a sequence of cations. The single significant $\text{C}-\text{H}\cdots\text{O}$ hydrogen bond (Table 2), which involves a $\text{C}-\text{H}$ bond adjacent to the charged N1, lies within the $(01\bar{1})$ sheet and hence does not influence the overall dimensionality of the supramolecular structure.

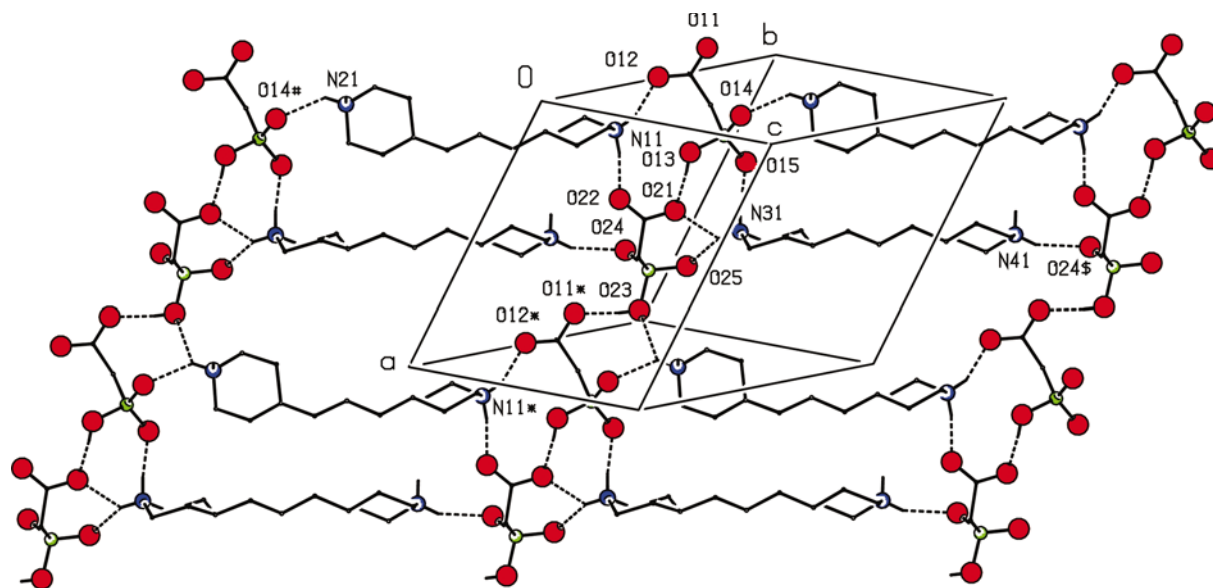


Figure 7

Part of the crystal structure of (3), which shows the formation of a $(01\bar{1})$ sheet generated by translation. For the sake of clarity, H atoms bonded to C atoms are omitted. The atoms marked with an asterisk (*), hash (#) or dollar sign (\$) are at the symmetry positions $(1 + x, y, z)$, $(x, -1 + y, -1 + z)$ and $(x, 1 + y, 1 + z)$, respectively.

3.3.4. The anions form chains of edge-fused rings (molecular ladders). In (5) (Fig. 12) the anions alone form a chain of fused rings. The cations link the anion chains into sheets by means of N—H...O hydrogen bonds, and these sheets are then linked to form three-dimensional structures by C—H...O hydrogen bonds. As in (4), both the phosphonate and the carboxyl groups in the anion of compound *D* are involved in the chain formation. The phosphonate O3 in the anion at (x, y, z) acts as hydrogen-bond donor to the phosphonate O4 in the anion at $(1 - x, 1 - y, 1 - z)$, so generating an $R_2^2(8)$ motif centred at $(\frac{1}{2}, \frac{1}{2}, \frac{1}{2})$. In addition, the carboxyl O1 in the anion at (x, y, z) acts as donor to the phosphonate O5 in the anion at $(-1 + x, y, z)$, so a $C(6)$ chain that runs parallel to $[100]$ is generated by translation. The combination of the two O—H...O hydrogen bonds generates a chain of fused centrosymmetric rings (Fig. 13) with $R_2^2(8)$ rings centred at $(n + \frac{1}{2}, \frac{1}{2}, \frac{1}{2})$ ($n = \text{zero or integer}$) and $R_4^4(20)$ rings centred at $(n, \frac{1}{2}, \frac{1}{2})$ ($n = \text{zero or integer}$).

By means of N—H...O hydrogen bonds, the cations link $[100]$ chains into a (001) sheet. The amino N1 acts as hydrogen-bond donor to the phosphonate O4 within the asymmetric unit (Fig. 12). This O4 atom lies in the anion chain along $(x, \frac{1}{2}, \frac{1}{2})$. In addition, the pyridinium N12 in the cation at (x, y, z) acts as donor to the phosphonate O5 in the anion at $(1 - x, -y, 1 - z)$. This O5 lies in the anion chain along $(x, -\frac{1}{2}, \frac{1}{2})$. These two N—H...O hydrogen bonds are propagated by inversion to form the (001) sheet (Fig. 14). Within this sheet, where the cations generate a sequence of alternating centrosymmetric $R_4^4(16)$ and $R_6^4(24)$ rings, pairs of cations form aromatic π ... π stacking interactions across the $R_4^4(16)$ rings. The rings, which contain N12 at (x, y, z) and N22 at $(1 - x, -y, 1 - z)$, are almost parallel, with an interplanar angle of only $8.8(2)^\circ$: the ring-centroid separation is $3.533(2)$ Å with an interplanar separation of *ca.* 3.3 Å.

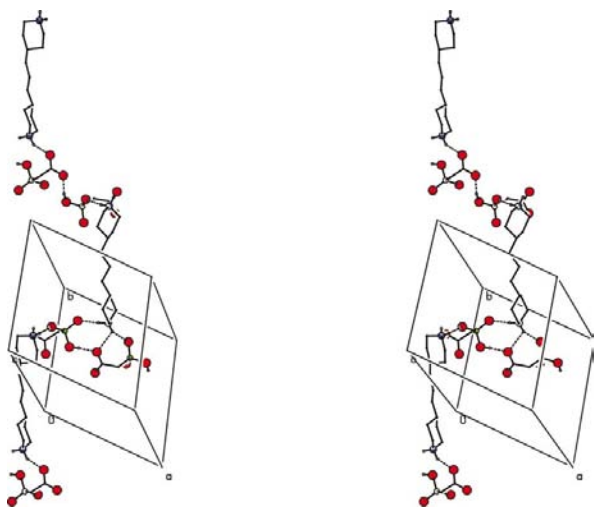


Figure 8

Stereoview of part of the structure of (3), which shows the formation of the $[021]$ chain that links the $(01\bar{1})$ sheets into a continuous framework. For the sake of clarity, H atoms bonded to C atoms are omitted.

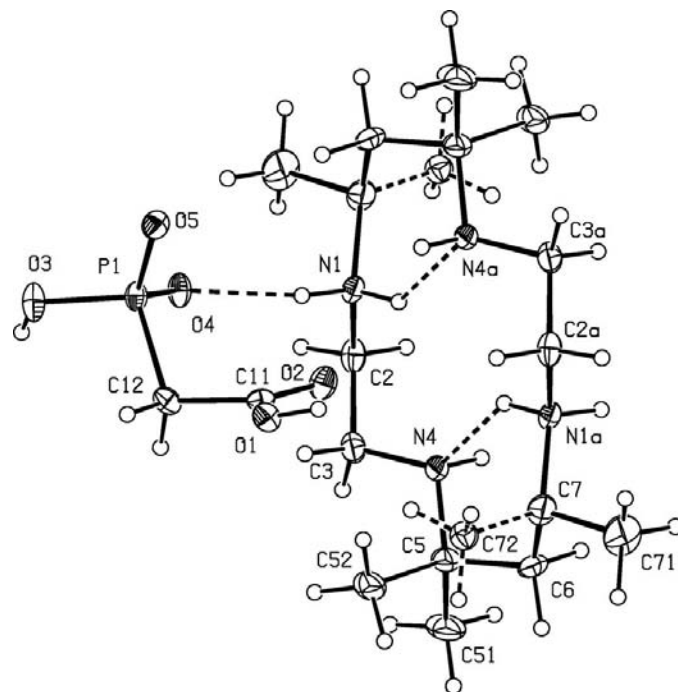


Figure 9

The molecular components of (4) and the atom-labelling scheme. Displacement ellipsoids are drawn at the 30% probability level. The atoms marked 'a' are at the symmetry position $(1 - x, 1 - y, 1 - z)$. The methyl groups that contain C52 and C72 have occupancies 0.679 (5) and 0.321 (5), respectively.

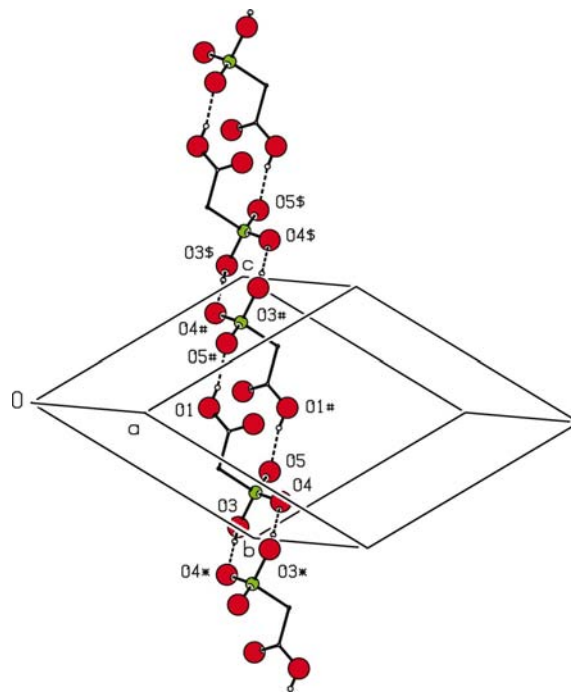


Figure 10

Part of the crystal structure of (4), which shows the formation of a chain of anions along $[01\bar{1}]$. This chain contains spiro-fused $R_2^2(8)$ and $R_2^2(12)$ rings. For the sake of clarity, H atoms bonded to C atoms are omitted. The atoms marked with an asterisk (*), hash (#) or dollar sign (\$) are at the symmetry positions $(-x, 2 - y, -z)$, $(-x, 1 - y, 1 - z)$ and $(x, -1 + y, 1 + z)$, respectively.

The (001) sheets are linked by a single, rather weak C—H...O hydrogen bond. C24 in the cation at (x, y, z) lies in the sheet centred at $z = 0.5$, and C24 acts as hydrogen-bond donor to the carboxyl O2 in the anion at $(1 + x, y, 1 + z)$, which is a component of the (001) sheet centred at $z + \frac{1}{2}$. Propagation

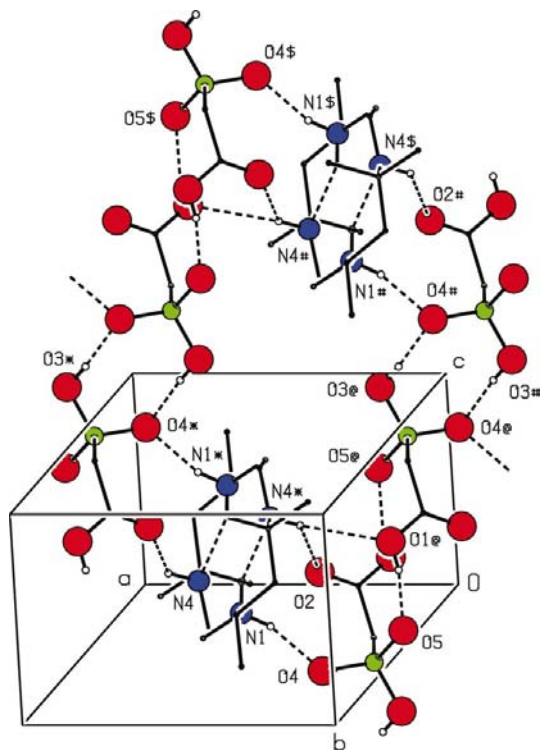


Figure 11

Part of the crystal structure of (4), which shows the linking of the $[01\bar{1}]$ anion chains by the centrosymmetric cations. For the sake of clarity, H atoms bonded to C atoms are omitted, and only the major orientation of the cation is shown. The atoms marked with an asterisk (*), hash (#), dollar sign (\$) or at sign (@) are at the symmetry positions $(1 - x, 1 - y, 1 - z)$, $(x, -1 + y, 1 + z)$, $(1 - x, -y, 2 - z)$ and $(-x, 1 - y, 1 - z)$, respectively.

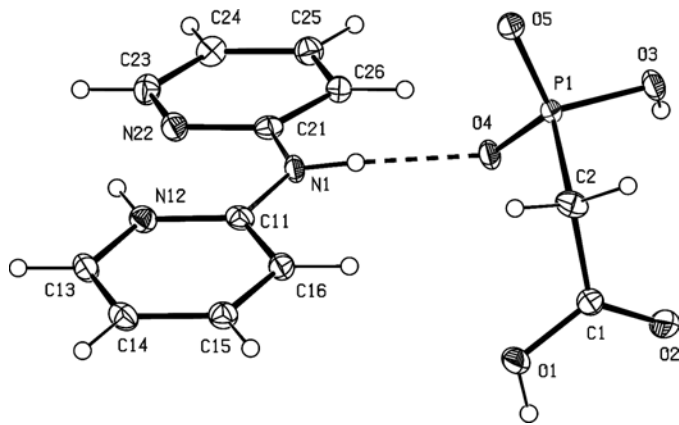


Figure 12

The molecular components of (5) and the atom-labelling scheme. Displacement ellipsoids are drawn at the 30% probability level. For the sake of clarity, only the major orientation of the cation is shown.

of this hydrogen bond links all of the sheets into a single three-dimensional framework.

3.3.5. The anion substructure is two-dimensional. *Compound (6).* The anion substructure in (6) (Fig. 15) is two-dimensional and thus entirely different from the anion substructures in (1)–(5). However, it is readily analysed in terms of a dimeric unit analogous to a fragment of the anion substructure in (4). The carboxyl O1 in the anion at (x, y, z) acts as hydrogen-bond donor to the phosphonate O4 in the anion at $(1 - x, 1 - y, 1 - z)$; thus a centrosymmetric $R_2^2(12)$ motif is generated, which is centred at $(\frac{1}{2}, \frac{1}{2}, \frac{1}{2})$. The same $R_2^2(12)$ motif occurs in (4). However, instead of being linked to just two other similar units, as in (4) (Fig. 10), in (6) each of the $R_2^2(12)$ units is linked to four others (Fig. 16), and this is the basis of the anion sheet formation.

In the dimeric anion unit centred at $(\frac{1}{2}, \frac{1}{2}, \frac{1}{2})$, the phosphonate O3 atoms at (x, y, z) and $(1 - x, 1 - y, 1 - z)$ act as hydrogen-bond donors, respectively, to the phosphonate O5 atoms in the anions at $(x, \frac{1}{2} - y, -\frac{1}{2} + z)$ and $(1 - x, \frac{1}{2} + y,$

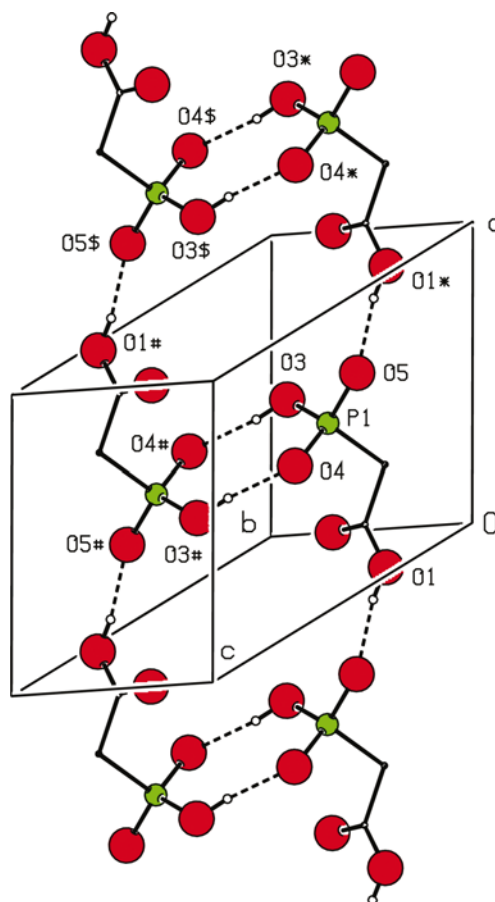


Figure 13

Part of the crystal structure of (5), which shows the formation of a chain of anions along $[100]$. This chain contains fused $R_2^2(8)$ and $R_4^4(20)$ rings. For the sake of clarity, H atoms bonded to C atoms are omitted. The atoms marked with an asterisk (*), hash (#) or dollar sign (\$) are at the symmetry positions $(1 + x, y, z)$, $(1 - x, 1 - y, 1 - z)$ and $(2 - x, 1 - y, 1 - z)$, respectively.

$\frac{3}{2} - z$), respectively, which themselves are components of the $R_2^2(12)$ units centred at $(\frac{1}{2}, 0, 0)$ and $(\frac{1}{2}, 1, 1)$, respectively. In like manner, the two phosphonate O5 atoms in the $(\frac{1}{2}, \frac{1}{2}, \frac{1}{2})$ dimer accept hydrogen bonds from atoms O3 at $(x, \frac{1}{2} - y, \frac{1}{2} + z)$ and $(1 - x, \frac{1}{2} + y, \frac{1}{2} - z)$, which themselves lie in the $R_2^2(12)$ units centred at $(\frac{1}{2}, 0, 1)$ and $(\frac{1}{2}, 1, 0)$, respectively. In this way, an anion sheet parallel to (100) is generated in which $R_2^2(12)$ and $R_2^2(28)$ rings alternate in checkerboard fashion (Fig. 16).

Within the asymmetric unit (Fig. 15), N11 acts as hydrogen-bond donor to the phosphonate O4: with the reference anion sheet centred at $x = \frac{1}{2}$, the cation is thus centred at $(0, 0, \frac{1}{2})$. The symmetry-related N11 in this cation lies at $(-x, -y, 1 - z)$ and acts as donor to O4 in the anion at $(-x, -y, 1 - z)$. This O4 is a component of the $R_2^2(12)$ unit centred at $(-\frac{1}{2}, -\frac{1}{2}, \frac{1}{2})$, which itself lies in the anion sheet centred at $x = \frac{1}{2}$ (Fig. 17). Hence the cations link each anion sheet to its two neighbours, so that the three-dimensional framework can be generated by the hard hydrogen bonds alone.

However, the linking of the (100) sheets is reinforced by three C—H...O hydrogen bonds (Table 2), so that each centrosymmetric cation acts as a sixfold donor in such bonds. In the cation centred at $(0, 0, \frac{1}{2})$, atoms C13 at (x, y, z) and C15 at $(-x, -y, 1 - z)$ both act as hydrogen-bond donors to O3 in the anion at $(1 - x, -\frac{1}{2} + y, \frac{1}{2} - z)$, while C16 at (x, y, z) acts as donor to O2 in the anion at $(1 - x, 1 - y, 1 - z)$. These two

anions are both components of the anion sheet centred at $x = \frac{1}{2}$. The symmetry-related C atoms in the $(0, 0, \frac{1}{2})$ cation act as hydrogen-bond donors to the anions at $(-1 + x, \frac{1}{2} - y, \frac{1}{2} + z)$ and $(-1 + x, -1 + y, z)$, which both lie in the anion sheet centred at $x = -\frac{1}{2}$ (Fig. 18).

The N,N'-dimethylpiperazine adduct at 150 (1) K. In the 1:2 salt formed between N,N'-dimethylpiperazine and phosphonoacetic acid it is observed that, at 293 (2) K, the H atoms that are bonded to O atoms are disordered (Farrell *et al.*, 2001). We have therefore reinvestigated this compound at 150 (1) K. This reinvestigation shows that the structures at the two temperatures are effectively identical, aside from the expected

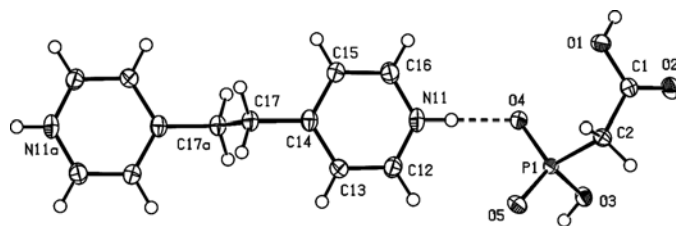


Figure 15

The molecular components of (6) and the atom-labelling scheme. Displacement ellipsoids are drawn at the 30% probability level. The atoms marked 'a' are at the symmetry position $(-x, -y, 1 - z)$.

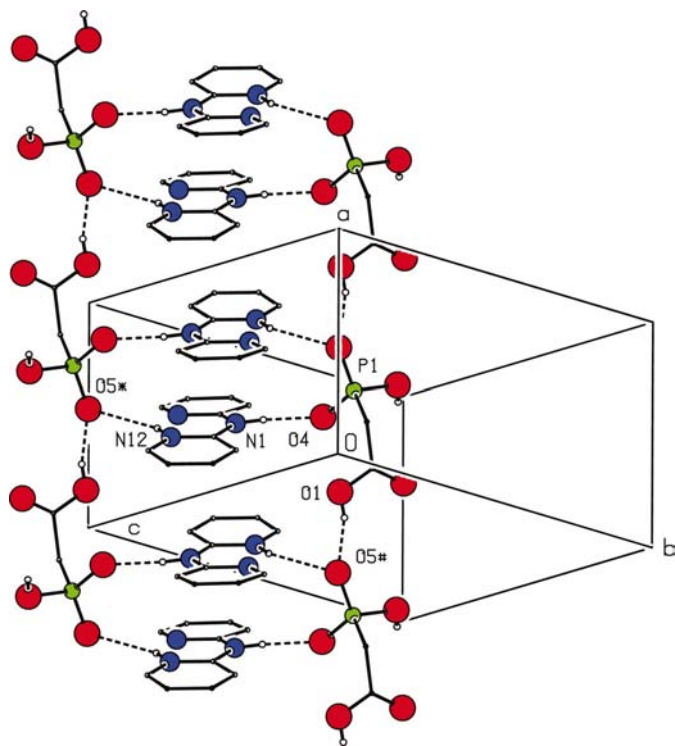


Figure 14

Part of the crystal structure of (5), which shows the linking of the [100] anion chains by the cations and the $\pi \cdots \pi$ stacking of the cations. For the sake of clarity, H atoms bonded to C atoms are omitted, as is the intramolecular N—H...N hydrogen bond. The atoms marked with an asterisk (*) or hash (#) are at the symmetry positions $(1 - x, -y, 1 - z)$ and $(-1 + x, y, z)$, respectively.

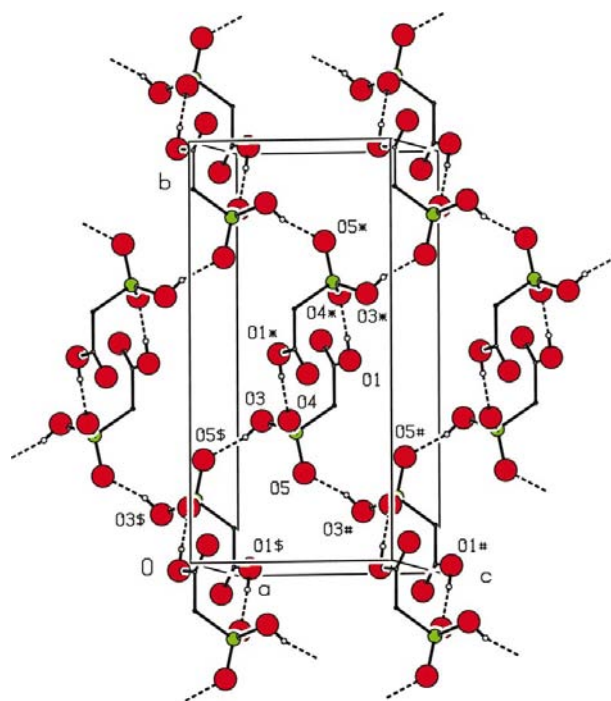


Figure 16

Part of the crystal structure of (6), which shows the formation of a (100) sheet of anions built from alternating $R_2^2(12)$ and $R_2^2(28)$ rings. For the sake of clarity, H atoms bonded to C atoms are omitted. The atoms marked with an asterisk (*), hash (#) or dollar sign (\$) are at the symmetry positions $(1 - x, 1 - y, 1 - z)$, $(x, \frac{1}{2} - y, -\frac{1}{2} + z)$ and $(x, \frac{1}{2} - y, \frac{1}{2} + z)$, respectively.

changes in the unit-cell parameters, and, in particular, that the H atoms bonded to O atoms are still disordered at 150 (1) K.

3.3.6. General comments on the substructures. The acid substructures in compounds (1)–(3) are in the form of simple chains and are dominated by the $C(4)$ motif [$C_2^2(8)$ in (3) where there are two independent anions], which is a characteristic feature of both simple phosphonic acids (Weakley, 1976; Lis, 1997) and simple aliphatic carboxylic acids (Jones & Templeton, 1958; Nahrungbauer, 1970; Jönsson, 1971). This motif can also be identified within the sheet substructure in (6). However, while the $R_2^2(8)$ phosphonate motif that is present in phenylphosphonic acid (Weakley, 1976) is also present in both (4) and (5), the $R_2^2(8)$ carboxyl motif that is

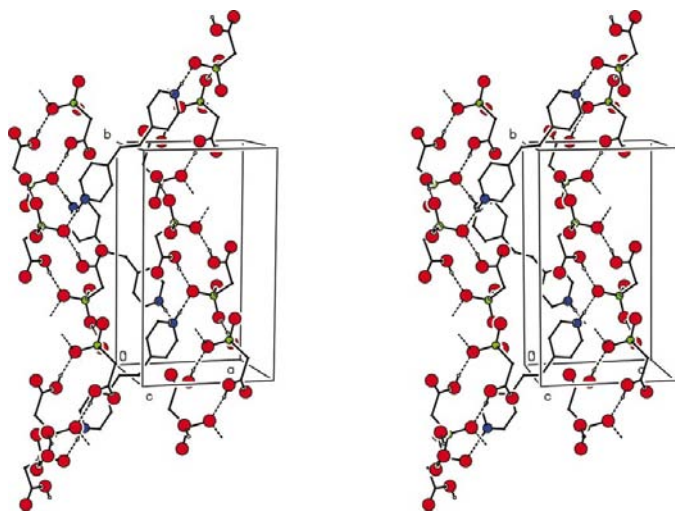


Figure 17
Stereoview of part of the crystal structure of (6), which shows the linking of the (100) anion sheets by the cations. For the sake of clarity, H atoms bonded to C atoms are omitted.

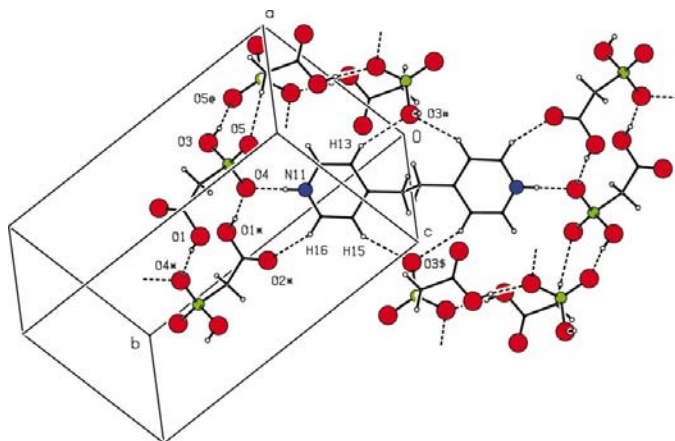


Figure 18
Part of the crystal structure of (6), which shows the C–H...O hydrogen bonds that link the (100) anion sheets. The atoms marked with an asterisk (*), hash (#), dollar sign (\$) or at sign (@) are at the symmetry positions $(1-x, 1-y, 1-z)$, $(1-x, -\frac{1}{2}+y, \frac{1}{2}-z)$, $(-1+x, \frac{1}{2}-y, \frac{1}{2}+z)$ and $(x, \frac{1}{2}-y, -\frac{1}{2}+z)$, respectively.

characteristic of many carboxylic acids is absent throughout. The mixed phosphonic/carboxylic $R_2^2(12)$ motif, which is also present in pure phosphonoacetic acid (Lis, 1997), is observed only in (4) and (6). Hence the hydrogen-bonding patterns in the acid substructures vary substantially within this series, and these variations alone pose a real challenge to methods aimed at the computation from first principles of the crystal structures of molecular systems.

4. Concluding comments

The results reported here, for a series of adducts formed by a single acid with a range of rather simple and closely related amines, encompass a wide variety of molecular constitutions and supramolecular arrangements. The nature of the acid components, whether neutral species, mono-anions or di-anions, is not readily predictable: for example, while there is no proton transfer to the DABCO units in (1), so that the phosphonoacetic acid unit is neutral, in the related adduct of DABCO with *N*-(phosphonomethyl)iminodiacetic acid the DABCO unit is doubly protonated, so that the other component is a di-anion (Bowes *et al.*, 2002). Similarly, the acid substructures exhibit wide variation. Taken together, these two properties mean that no one supramolecular structure can readily be predicted, even with detailed foreknowledge of all the others in the series. This fact in turn may mean that attempts to apply simple principles of crystal engineering to the design and construction of specific supramolecular structures in systems such as those described here will require considerably more sophisticated predictive models than are currently available.

X-ray data were collected at the University of Toronto using a Nonius Kappa-CCD diffractometer purchased with funds from NSERC Canada.

References

- Allen, F. H. & Kennard, O. (1993). *Chem. Des. Autom. News*, **8**, 1/31–37.
- Barefield, E. K., Bianchi, A., Billo, E. J., Connolly, P. J., Paoletti, P., Summers, J. S. & Van Derveer, D. G. (1986). *Inorg. Chem.* **25**, 4197–4202.
- Bowes, K. F., Ferguson, G., Glidewell, C. & Lough, A. J. (2002). *Acta Cryst.* **C58**, o467–o469.
- Braga, D., Grepioni, F., Biradha, K., Pedireddi, V. R. & Desiraju, G. R. (1995). *J. Am. Chem. Soc.* **117**, 3156–3166.
- Farrell, D. M. M., Ferguson, G., Lough, A. J. & Glidewell, C. (2001). *Acta Cryst.* **C57**, 952–954.
- Ferguson, G. (1999). *PRPKAPPA. A WordPerfect 5.1 Macro to Formulate and Polish CIF Format Files from the SHELXL97 Refinement of Kappa-CCD Data*. University of Guelph, Canada.
- Ferguson, G., Glidewell, C., Gregson, R. M. & Meehan, P. (1998). *Acta Cryst.* **B54**, 129–138.
- Gregson, R. M., Glidewell, C., Ferguson, G. & Lough, A. J. (2000). *Acta Cryst.* **B56**, 39–57.
- Jones, R. E. & Templeton, D. H. (1958). *Acta Cryst.* **11**, 484–487.
- Jönsson, P.-G. (1971). *Acta Cryst.* **B27**, 893–898.
- Lis, T. (1997). *Acta Cryst.* **C53**, 28–42.
- Nahrungbauer, I. (1970). *Acta Chem. Scand.* **24**, 453–462.

- Nonius (1997). *Kappa-CCD Server Software*. Windows 3.11 Version. Nonius BV, Delft, The Netherlands.
- Otwinowski, Z. & Minor, W. (1997). *Methods Enzymol.* **276**, 307–326.
- Sheldrick, G. M. (1997*a*). *SHELXL97. Program for the Refinement of Crystal Structures*. University of Göttingen, Germany.
- Sheldrick, G. M. (1997*b*). *SHELXS97. Program for the Solution of Crystal Structures*. University of Göttingen, Germany.
- Spek, A. L. (2003). *J. Appl. Cryst.* **36**, 7–13.
- Weakley, T. J. R. (1976). *Acta Cryst.* **B32**, 2889–2890.
- Wilson, A. J. C. (1976). *Acta Cryst.* **A32**, 994–996.
- Yokozeki, A. & Kuchitsu, K. (1971). *Bull. Chem. Soc. Jpn.*, **44**, 72–77.